computation

MDPI

Article

Numerical Simulation of Cytokinesis Hydrodynamics

Andriy A. Avramenko [1], Igor V. Shevchuk [2,*], Andrii I. Tyrinov [1] and Iryna V. Dzevulska [3]

[1] Institute of Engineering Thermophysics, National Academy of Sciences, 03057 Kiev, Ukraine; tgetu.ittf@gmail.com (A.A.A.)
[2] Faculty of Computer Science and Engineering Science, TH Köln—University of Applied Sciences, 51643 Gummersbach, Germany
[3] Department of Descriptive and Clinical Anatomy, Bogomolets National Medical University, 01601 Kiev, Ukraine; dzevulska@gmail.com
* Correspondence: igor_v.shevchuk@th-koeln.de

Abstract

A hydrodynamic homogeneous model has been developed for the motion of mutually impenetrable viscoelastic non-Newtonian fluids taking into account surface tension forces. Based on this model, numerical simulations of cytokinesis hydrodynamics were performed. The cytoplasm is considered a non-Newtonian viscoelastic fluid. The model allows for the calculation of the formation and rupture of the intercellular bridge. Results from an analytical analysis shed light on the influence of the viscoelastic fluid's relaxation time on cytokinesis dynamics. A comparison of numerical simulation results and experimental data showed satisfactory agreement.

Keywords: cytokinesis; numerical modeling; hydrodynamics; non-Newtonian viscoelastic fluid; intercellular bridge

Academic Editor: Sergey A. Karabasov

Received: 29 May 2025
Revised: 24 June 2025
Accepted: 4 July 2025
Published: 8 July 2025

Citation: Avramenko, A.A.; Shevchuk, I.V.; Tyrinov, A.I.; Dzevulska, I.V. Numerical Simulation of Cytokinesis Hydrodynamics. *Computation* **2025**, *13*, 163. https://doi.org/10.3390/computation13070163

1. Introduction

Cytokinesis is not just the final stage of cell division, but a fundamental process that ensures proper reproduction, growth, and maintenance of tissue, genetic stability, and development of multicellular organisms. Disturbances in this process can lead to various pathologies, including cancer and developmental defects. The article [1] is devoted to modeling cell cytokinesis while taking morphology into account. It describes a three-dimensional (3D) fluid flow model of eukaryotic cell cytokinesis. The active force of actomyosin along the cytokinetic ring is modeled by the surface force, while the cell morphology is tracked using the phase field model.

A model that can explain the location of furrows in very large cells is proposed in [2]. The model correctly predicts the location and appearance of furrows in two experiments in which the cell shape is changed to an hourglass or cylindrical shape before division. These results are consistent with theories of equatorial stimulation, but are inconsistent with models that require differential stimulation of the polar regions of the cell without furrows.

In ref. [3], it was shown that during cytokinesis, contractility factors accumulate near the furrow in adjacent cells. Increased stiffness in neighboring cells slows down furrow formation, while increased contractility in one or both neighboring cells either slows down furrow formation or induces cytokinetic failure. Computational modeling confirms these findings and provides additional insight into the mechanics of the epithelium during cytokinesis.

In ref. [4], a novel unfitted finite element framework is presented for modeling coupled surface and bulk problems in time-dependent domains, focusing on fluid–fluid interactions

in animal cells between the actomyosin cortex and the cytoplasm. This approach ensures accurate and stable simulations on fixed Cartesian grids.

An important point for modern biotechnology is the understanding of bioconvection processes [5,6], processes occurring in neural systems [7–10], and processes occurring during cell division. The final stage of cell division, when the bridge connecting two daughter cells thins and breaks, is called cytokinesis. Experimental data indicate that cytokinesis disorders lead to multiple intercellular bridges and multinuclear cells [11] and threaten their genomic and cellular integrity. The appearance of such "defective" cells can cause, for example, oncological diseases.

Fluid flow modeling during cytokinesis using a one-dimensional model was performed in [12].

Theoretical and numerical study of mass transfer can serve as a guide for experimentalists regarding the values of those properties that should be measured in order to provide more accurate answers to questions regarding the dynamics of cell cytokinesis. The connection between defective cytokinesis and various diseases provides a strong incentive for research in this area.

In this paper, numerical and analytical modeling of fluid flow modeling during cytokinesis is performed without taking into account the internal structure of the cell.

2. Statement of the Problem

For the first time, a combination of the VOF (Volume of Fluid) method with the Oldroyd-B non-Newtonian fluid model is proposed for modeling intracellular hydrodynamics. The model can be used to assess the nature of cytokinesis without considering the influence of the cell's internal elements.

The physical statement of the problem and the schematic of the computational domain are shown in Figure 1. Two mutually penetrating spherical drops of cytoplasm (non-Newtonian fluid) are located in the external environment. The dimensions of the computational domain were $30 \cdot 10^{-6} \times 8 \cdot 10^{-6}$ m. The radii R of the drops at the initial moment are equal to $4 \cdot 10^{-6}$ m. At the initial moment of time, the initial volumes of liquid move as follows: volume 2 is stationary, and volumes 1 and 3 move in opposite directions with the same velocity v_0, equal to $1.2 \cdot 10^{-6}$ m/s along the axis of symmetry z. The remaining regions have zero velocity.

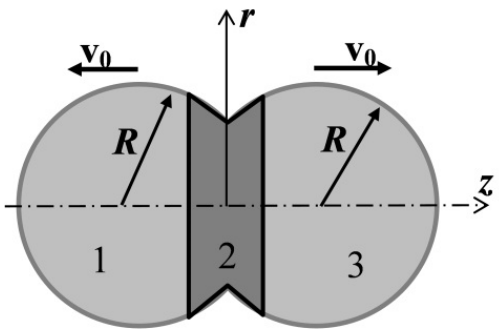

Figure 1. Computational domain for modeling of cytokinesis.

Numerical calculations were performed in an axisymmetric statement for a non-Newtonian viscoelastic fluid. The VOF (Volume of Fluid) model was used, in which the liquids are mutually non-penetrating. This model takes into account the surface tension

forces at the interface between the liquids. The equations for momentum transfer and continuity in the axial (z) and radial (r) directions for this model are as follows [13]

$$\begin{array}{l} \frac{\partial}{\partial t}(\rho v_z) + \frac{1}{r}\frac{\partial}{\partial z}(r\rho v_z v_z) + \frac{1}{r}\frac{\partial}{\partial r}(r\rho v_r v_z) = -\frac{\partial p}{\partial z} + \frac{2}{r}\frac{\partial}{\partial z}(r\tau_{zz}) + \frac{1}{r}\frac{\partial}{\partial r}(r\tau_{zr}) + F_z, \\ \frac{\partial}{\partial t}(\rho v_r) + \frac{1}{r}\frac{\partial}{\partial z}(r\rho v_z v_r) + \frac{1}{r}\frac{\partial}{\partial r}(r\rho v_r v_r) = -\frac{\partial p}{\partial r} + \frac{1}{r}\frac{\partial}{\partial z}(r\tau_{rz}) + \frac{2}{r}\frac{\partial}{\partial r}(r\tau_{rr}) + F_r, \\ \frac{\partial \rho}{\partial t} + \frac{\partial \rho v_z}{\partial z} + \frac{\partial \rho v_r}{\partial r} + \frac{\rho v_r}{r} = 0. \end{array} \quad (1)$$

The relation between the stress and strain rate tensors for a non-Newtonian fluid is as follows (Oldroyd-B model) [14]:

$$\lambda\frac{\partial T}{\partial t} + T = 2\mu\left(D + \gamma\frac{\partial D}{\partial t}\right), \quad (2)$$

where T is the stress tensor,

$$T = \begin{Bmatrix} \tau_{zz} & \tau_{zr} \\ \tau_{rz} & \tau_{rr} \end{Bmatrix}. \quad (3)$$

Tensor D has the following form

$$D = \begin{Bmatrix} \frac{\partial v_r}{\partial r} & \frac{1}{2}\left(\frac{\partial v_z}{\partial r} + \frac{\partial v_r}{\partial z}\right) \\ \frac{1}{2}\left(\frac{\partial v_r}{\partial z} + \frac{\partial v_z}{\partial r}\right) & \frac{\partial v_z}{\partial z} \end{Bmatrix}. \quad (4)$$

The density ρ in Equation (1) is calculated using the following equation

$$\rho = \varphi_2\rho_2 + (1 - \varphi_2)\rho_1, \quad (5)$$

where φ_1 are φ_2 are the volume fractions of the external environment and cytoplasm in the computational cell, ρ_2 is the cytoplasm density, and ρ_1 is the external environment density.

To compare the numerical results with the experimental data, the parameters of cytoplasm from [11] were used in the numerical modeling (see Table 1).

Table 1. Parameters of cytoplasm.

Cytoplasm density	1000 kg/м^3
Cytoplasm viscosity	350 Pa·s
Cytoplasm relaxation time	28 s
Speed of movement of the spherical part of the cell	$1.2{\cdot}10^{-6}$ m/s

The VOF model used is based on the assumption that the phases under study (in this case, the cell cytoplasm and the external environment) do not interpenetrate. A variable is introduced into the model, which represents the volume fraction of the cytoplasm in the computational cell. In each cell, the sum of the volume fractions of the cytoplasm and the external environment is equal to one. Thus, the values of the variables in any cell determine the current amount of cytoplasm depending on its volume value.

The interface between the cytoplasm and the external environment is determined in accordance with the solution of the continuity equations for the volume fractions of the cytoplasm φ_2 and the external environment φ_1. These equations have the following form:

$$\begin{array}{l} \frac{\partial \varphi_1}{\partial t} + \mathbf{v}\cdot\mathrm{grad}(\varphi_1) = 0, \\ \frac{\partial \varphi_2}{\partial t} + \mathbf{v}\cdot\mathrm{grad}(\varphi_2) = 0, \\ \varphi_1 + \varphi_2 = 1. \end{array} \quad (6)$$

Here, F_z and F_r in Equation (1) are the axial and radial components of the force, respectively, taking into account the surface tension [15]

$$F = \sigma \frac{\rho k \, \mathrm{grad}(\varphi_2)}{\frac{1}{2}(\rho_1 + \rho_2)}, \tag{7}$$

where σ is the surface tension at the interface between the cytoplasm and the external environment, and the curvature of the interface k is determined as follows [15]

$$k = \mathrm{div}(\hat{n}), \hat{n} = \frac{n}{|n|}, n = \mathrm{grad}(\varphi_2). \tag{8}$$

The following boundary conditions were used in the modeling:

- At the boundaries parallel to the axis of symmetry: $p = p_{atm}; \mathrm{v_z} = 0$;
- At the boundaries perpendicular to the axis of symmetry: $p = p_{atm}; \mathrm{v_r} = 0$.

The initial configuration of the cytoplasm is specified in the description of the problem statement. The working pressure is taken to be equal to one atmosphere.

Calculations of stress tensors and strain rates for a non-Newtonian fluid according to Equations (2)–(4) were implemented in the form of UDFs (user-defined functions).

The time step of the model was 10^{-15} s.

Numerical simulations were performed using ANSYS Fluent 6.0.

3. Results of Numerical Modeling

The shape of the cytoplasm surface obtained during modeling for different moments in time is presented in Figure 2.

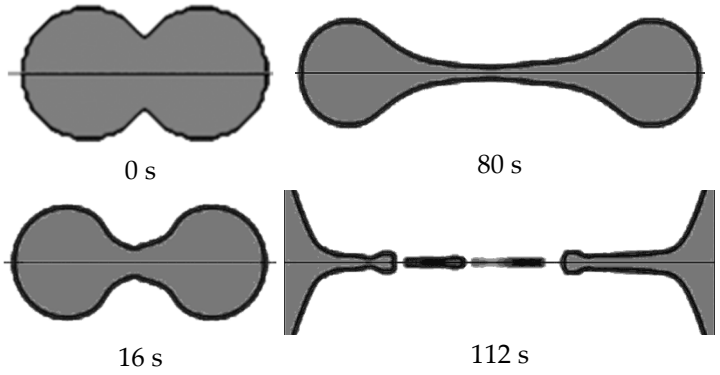

Figure 2. Results of numerical modeling of the cytokinesis process for different moments in time.

When regions 1 and 3 diverge (Figure 1), the diameter of region 2 decreases under the action of the surface tension force. In this case, an intercellular bridge is formed. With further divergence, the resulting bridge lengthens and becomes thinner. Up to time t = 60 s, the diameter of the intercellular bridge varies significantly in length. The minimum diameter at this time is located in its middle. At subsequent times, the shape of the bridge becomes almost cylindrical along its entire length. The rate of thinning decreases as the bridge diameter decreases. Having reached the minimum critical diameter (at the time t = 112 s), the bridge connecting the diverging regions breaks. Subsequently, the remains of the bridge are drawn into the formed volumes under the action of the surface tension force.

Based on the results of numerical studies, the dependences of the diameter and length of the intercellular bridge on time are plotted in Figure 3. The same figure shows the experimental dependences from [11]. The figure shows good agreement between the numerical and experimental results. The calculated and experimental data show that the

length and diameter of the intercellular bridge change according to a law that is close to linear.

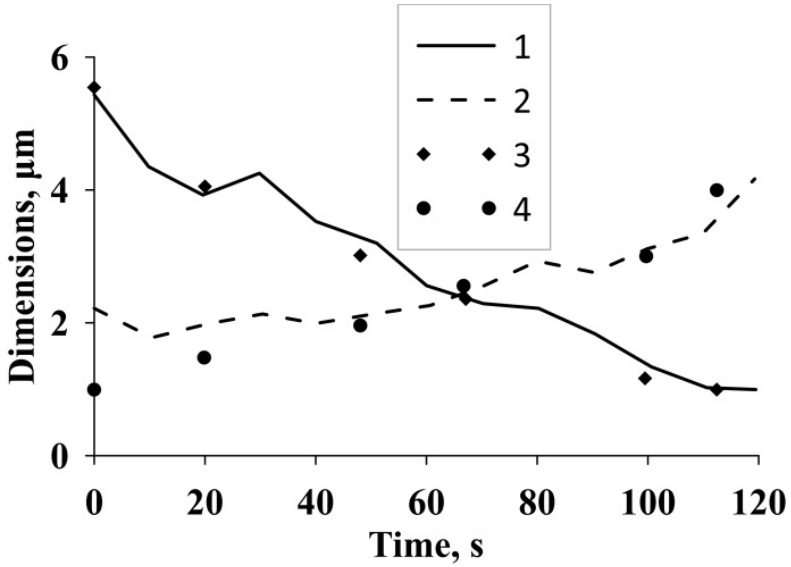

Figure 3. Dependences of the diameter and length of the intercellular bridge on time: 1—diameter [11]; 2—length [11]; 3—diameter (calculation); 4—length (calculation).

4. Analytic Analysis

For an approximate qualitative analysis, we consider Equation (2) as an unsteady differential equation with respect to the stress tensor. In this case, we will consider the strain rate tensor as a given function of time

$$\frac{dT}{dt} + \frac{T}{\lambda} = \frac{\mu}{\lambda}\left(D + \gamma\frac{dD}{dt}\right) = f(t). \tag{9}$$

The initial condition for this equation is

$$T = 0 \qquad \text{При} \qquad t = 0. \tag{10}$$

For the analytical solution of this equation, we use the method of separation of functions, i.e., we will look for a solution in the following form

$$T(t) = u \cdot w. \tag{11}$$

Substituting Equation (9) into Equation (11) yields

$$w\frac{du}{dt} + u\frac{dw}{dt} + \frac{uw}{\lambda} = w\frac{du}{dt} + u\left(\frac{dw}{dt} + \frac{w}{\lambda}\right) = f(t). \tag{12}$$

Since the functions u and w are arbitrary, they can be chosen so that the coefficient at u equals to zero. From here, we have

$$\frac{dw}{dt} + \frac{w}{\lambda} = 0. \tag{13}$$

$$w = \exp\left(-\frac{t}{\lambda}\right). \tag{14}$$

Next, we substitute Equation (14) into Equation (12) and integrate. This gives

$$u = \int_0^t f(t) \exp\left(\frac{t}{\lambda}\right) dt + C, \tag{15}$$

where C is the integration constant.

The final solution for the stress tensor is

$$T = \exp\left(-\frac{t}{\lambda}\right)\left(\int_0^t f(t) \exp\left(\frac{t}{\lambda}\right) dt + C\right). \tag{16}$$

Let us consider two special cases. The first one is when the deformation rates increase according to a linear law

$$D = A \cdot t, \tag{17}$$

where A is a constant.

Substitution of Equation (17) into Equation (16) yields the law of variation of stresses over time

$$T_1 = \tau + (g - 1)(1 - \exp(-\tau)), \tag{18}$$

where

$$T_1 = \frac{T}{A\lambda\mu}, \quad g = \frac{\gamma}{\lambda}, \quad \tau = \frac{t}{\lambda}. \tag{19}$$

Analysis of Equation (18) shows that the behavior of function T_1 depends on the sign of the value $g - 1$. If, i.e., when $\gamma > \lambda$, at small values of τ, a sharp increase in stress is observed (curve 4 on Figure 4); that is, the convexity of the curve is directed upward. This is due to the rapid increase in the deformation rate. Under the condition $\gamma < \lambda$, the opposite picture is observed (curve 2 on Figure 4). However, at large values of τ, regardless of the value of the parameter g, the increase in stress is linear. In the case of $g = 1$, it follows from Equation (18) that the process of cytokinesis obeys a linear law, as shown in curve 3 on Figure 3. As was said above, according to [15] the values of the parameters γ and λ tend to equality. Therefore, it is obvious that the most probable scenario of cytokinesis is described by Equation (18) under the condition $g \to 1$, i.e., it is linear.

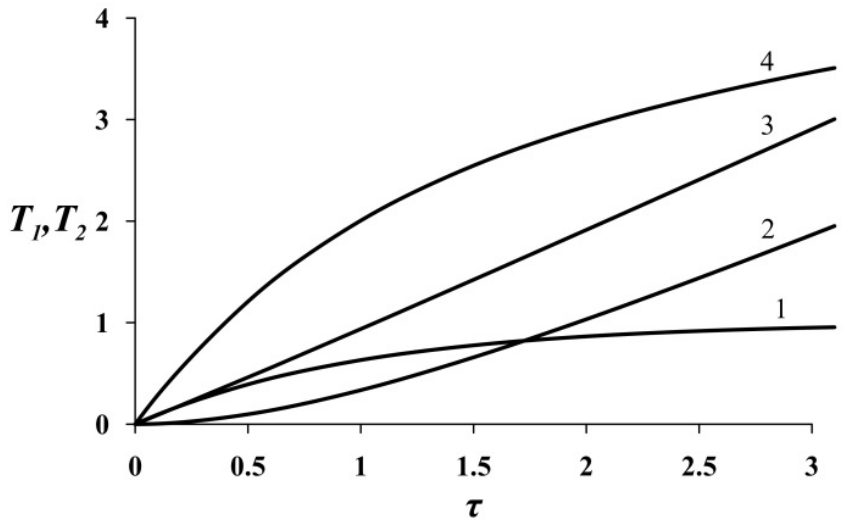

Figure 4. Variation of the stress tensor in time (curves (18) and (20)): 1—Heaviside function (20); 2—$\gamma < \lambda$ (18); 3—$g = 1$ (18); 4—$\gamma > \lambda$ (18).

The second case is when the deformation rates emerges as a Heaviside function $H(t)$, i.e., instantly,

$$D = A \cdot H(t). \tag{20}$$

At the same time,

$$\frac{dD}{dt} = \delta(t),$$

where $\delta(t)$ is the Dirac delta function. In this case, solution (15) takes the following form

$$T_2 = H(\tau) + \exp(-\tau)[(g-1)H(\tau) - gH(0)] \tag{21}$$

where

$$T_2 = \frac{T}{A\mu}. \tag{22}$$

This dependence is also shown in Figure 4 (curve 1). There is a linear section of increasing stress, after which an asymptote close to the horizontal line appears. Therefore, Equation (21) can describe cytokinesis at an early stage.

5. Conclusions

A homogeneous model of mutually non-penetrating fluids was proposed for the numerical simulation of cytokinesis hydrodynamics, which takes into account surface tension forces at their interface. A viscoelastic non-Newtonian fluid model was used to determine closure relations. This model allows us to trace the formation and rupture of the intercellular bridge that forms during cytokinesis.

Comparison of the numerical simulation results and experimental data [11] showed their satisfactory agreement. This indicates that the model used adequately describes fluid flow during cytokinesis. The differences in the size of the intercellular bridge at the initial time points are explained by the difference in the initial configuration of the cytoplasm from the real shape of the cell during cytokinesis.

Computational and experimental data show that the length and diameter of the intercellular bridge vary according to a law close to linear, although the properties of the cytoplasm differ from a linear law.

Comparison of numerical and analytical calculations shows that the most probable scenario of cytokinesis can be described by the Oldroyd-B model under the condition $g \to 1$. In this case, the diameter and length of the intercellular bridge change according to a law close to linear, which corresponds to the conclusion of [15].

In the future, we plan to conduct numerical studies of cytokinesis using other nonlinear models of viscoelastic non-Newtonian fluid.

Author Contributions: Conceptualization, A.A.A. and I.V.S.; Methodology, I.V.S., I.V.D. and A.I.T.; Software, A.I.T.; Validation, A.I.T. and I.V.D.; Formal analysis, A.A.A. and I.V.S.; Investigation, A.A.A., A.I.T. and I.V.S.; Data curation, A.I.T.; Writing—original draft preparation, A.A.A., I.V.S., I.V.D. and A.I.T.; Writing—review and editing, A.A.A., I.V.S. and A.I.T.; Visualization, A.A.A. and A.I.T. All authors have read and agreed to the published version of the manuscript.

Funding: The research contribution of authors A.A.A., A.I.T. and I.V.D. was funded in frames of the program of research projects of the National Academy of Sciences of Ukraine (No. 6541230) "Support of priority for the state scientific researches and scientific and technical (experimental) developments" 2023–2025 (1230). Project: "Development of technical principles for new high-efficient combustion technology of artificial fuels from solid household waste and biomass in cogeneration energy plants using hydrogen, oxygen, synthetic and biomethane to ensure energy safety."

Data Availability Statement: The original contributions presented in this study are included in the article. Further inquiries can be directed to the corresponding author.

Conflicts of Interest: The authors declare no conflicts of interest.

Abbreviation

φ	Volume fraction;
D	Strain rate tensor;
k	Surface curvature;
n	Normal to the surface;
p	Pressure;
t	Time;
v_r, v_z	Velocity components;
r, z	Coordinates;
F_r, F_z	Components of surface tension forces;
γ	Relaxation time for the strain tensor;
λ	Relaxation time of the stress tensor;
μ	Dynamic viscosity;
ρ	Density;
σ	Surface tension;
τ	Stress.

References

1. Zhao, J.; Wang, Q. Modeling Cytokinesis of Eukaryotic Cells Driven by the Actomyosin Contractile Ring. *Int. J. Numer. Methods Biomed. Eng.* **2016**, *32*, e02774. [CrossRef] [PubMed]
2. Devore, J.J.; Conrad, G.W.; Rappaport, R. A Model for Astral Stimulation of Cytokinesis in Animal Cells. *J. Cell Biol.* **1989**, *109*, 2225–2232. [CrossRef] [PubMed]
3. Landino, J.; Misterovich, E.; van den Goor, L.; Adhikary, B.; Chumki, S.; Davidson, L.A.; Miller, A.L. Neighbor cells restrain furrowing during *Xenopus* epithelial cytokinesis. *Dev. Cell* **2025**. [CrossRef] [PubMed]
4. Neiva, E.; Turlier, H. Unfitted finite element modelling of surface-bulk viscous flows in animal cells. *arXiv* **2025**, arXiv:2505.05723. [CrossRef]
5. Avramenko, A.A.; Kuznetsov, A.V. The Onset of Bio-thermal Convection in a Suspension of Gyrotactic Microorganisms in a Fluid Layer with an Inclined Temperature Gradient. *Int. J. Numer. Methods Heat Fluid Flow* **2010**, *20*, 111–129. [CrossRef]
6. Avramenko, A.A.; Kuznetsov, A.V. Bio-thermal Convection Caused by Combined Effects of Swimming of Oxytactic Bacteria and Inclined Temperature Gradient in a Shallow Fluid Layer. *Int. J. Numer. Methods Heat Fluid Flow* **2010**, *20*, 157–173. [CrossRef]
7. Kuznetsov, A.V.; Avramenko, A.A. Analytical Investigation of Transient Molecular-Motor-Assisted Transport in Elongated Cells. *Centr. Eur. J. Phys.* **2008**, *6*, 45–51. [CrossRef]
8. The Method of Separation of Variables for Solving Equations Describing Molecular-Motor-Assisted Transport of Intracellular Particles in a Dendrite or Axon. *Proc. R. Soc. A* **2008**, *464*, 2867–2886. [CrossRef]
9. Kuznetsov, A.V.; Avramenko, A.A. A Macroscopic Model of Traffic Jams in Axons. *Math. Biosci.* **2009**, *218*, 142–152. [CrossRef] [PubMed]
10. Kuznetsov, A.V.; Avramenko, A.A. A Minimal Hydrodynamic Model for a Traffic Jam in an Axon. *Int. Commun. Heat Mass Transf.* **2009**, *36*, 1–5. [CrossRef]
11. Zheng, F.; Basciano, C.; Li, J.; Kuznetsov, A.V. Fluid Dynamics of Cell Cytokinesis—Numerical Analysis of Intracellular Flow during Cell Division. *Int. Commun. Heat Mass Transf.* **2007**, *34*, 1–7. [CrossRef]
12. Kuznetsov, A.V.; Xiang, P. Numerical Investigation of Thinning of the Intercellular Bridge during Cell Cytokinesis. *Int. Commun. Heat Mass Transf.* **2006**, *33*, 1071–1078. [CrossRef]
13. Batchelor, G.K. *An Introduction to Fluid Dynamics*; Cambridge Mathematical Library; Cambridge University Press: Cambridge, UK, 2000; ISBN 978-0-521-66396-0.
14. Oldroyd, J.G. On the Formulation of Rheological Equations of State. *Proc. R. Soc. Lond. A* **1950**, *200*, 523–541. [CrossRef]
15. Brackbill, J.U.; Kothe, D.B.; Zemach, C. A Continuum Method for Modeling Surface Tension. *J. Comput. Phys.* **1992**, *100*, 335–354. [CrossRef]